Available online at www.sciencedirect.com
SCIENCE DIRECT®
Carbohydrate Research 339 (2004) 1447–1451
Carbohydrate RESEARCH

Solution and solid-state structure of *N*-acetamido-3,4,6-tri-*O*-acetyl-2-azido-2-deoxy-α-D-galactopyranosylamine

O. Srinivas,[a] B. Muktha,[b] S. Radhika,[a] T. N. Guru Row[b,*] and N. Jayaraman[a,*]

[a]*Department of Organic Chemistry, Indian Institute of Science, Bangalore 560 012, India*
[b]*Solid State and Structural Chemistry Unit, Indian Institute of Science, Bangalore 560 012, India*

Received 15 January 2004; revised 15 March 2004; accepted 27 March 2004

Abstract—High resolution ^{1}H NMR and ^{13}C NMR spectroscopic and single crystal X-ray structural analyses of *N*-acetamido-3,4,6-tri-*O*-acetyl-2-azido-2-deoxy-α-D-galactopyranosylamine (**1**), a minor product of azidonitration reaction of 3,4,6-tri-*O*-acetyl galactal, are reported. The solution phase studies of **1** reflect that the compound exists in $^{4}C_{1}$ conformation with *cis*-orientation of the substituents at C-1 and C-2. The solid-state structure of **1** reveals that a molecule of water is entrapped in the solid state of **1** and this water molecule serves to mediate N–H···O and C–H···O interactions.

Keywords: Azidonitration; Carbohydrates; Crystal structure; Hydrogen bonding; Weak interactions

1. Introduction

Lemieux and Ratcliffe have reported the elegant strategy of azidonitration of unsaturated pyranoses to derive 2-azido-2-deoxyglycosyl nitrates.[1] Since this report, the azidonitration reaction has been used extensively to prepare 2-deoxyglycosyl nitrates.[2] Azidonitration of an unsaturated glycopyranoside, namely the glycal, in MeCN solution, leads predominantly to afford the isomeric 2-azido-2-deoxyglycopyranosyl nitrates (Scheme 1). Formation of *N*-acetamido-2-azido-2-deoxy-α-D-galactopyranosylamine as a minor product of this reaction is observed commonly. The formation of this *N*-acetamido product enhances further when the reaction is carried out in aqueous MeCN.[1] The perception is that a 2-azido-2-deoxy-oxycarbonium ion intermediate allows attack by the solvent MeCN, the hydrolysis of the thus formed nitrilium intermediate leads to the acetamide substitution at the anomeric center.

During our efforts to synthesize glycopyranosyl azidonitrates as the precursor for 2-amino-2-deoxy-glycopyranosyl derivatives, we have performed azidonitration of 3,4,6-tri-*O*-acetyl galactal (**2**) (Scheme 1). As expected, a mixture of isomeric 2-azido-2-deoxy-3,4,6-tri-*O*-acetyl-α-D-galactopyranosyl-1-nitrates (75%) was obtained. Apart from these, the minor 2-azido-2-deoxy-α-D-galactopyranosyl amine (**1**) (~10%) was also

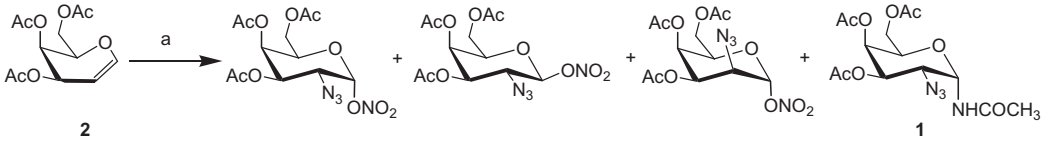

Scheme 1. Reagents and conditions: (a) ceric ammonium nitrate, NaN_3, CH_3CN.

* Corresponding authors. Tel.: +91-80-2293-2578/2406; fax: +91-80-2360-0529; e-mail: jayaraman@orgchem.iisc.ernet.in

0008-6215/$ - see front matter © 2004 Elsevier Ltd. All rights reserved.
doi:10.1016/j.carres.2004.03.025

isolated upon purification of the reaction mixture. Derivative **1** crystallized over a period of time from a solution of EtOAc–petroleum ether. In this report, we describe the single crystal X-ray structure of **1**, along with its solution phase characterization by ^{1}H and ^{13}C NMR spectroscopies. While the spectroscopic studies allowed us to ascertain the configurations and conformation of **1** in the solution phase, the crystal structure determination reveals the molecular properties and intermolecular interactions responsible for the stabilization of the crystal lattice. Specifically, the occurrence of a set of N–H···O and C–H···O, arising partly as a result of the incorporation of a molecule of water, stabilizes the molecular packing. The details of the solution and solid-state structural analyses of **1** are described herein.

2. Experimental

Derivative **1** was synthesized by adopting the procedure of Lemieux and Ratcliffe.[1] Spectral data for **1**: $[\alpha]_D$ +65.00 (*c* 2, $CHCl_3$) ^{1}H NMR (400 MHz, $CDCl_3$): δ 7.33 (d, $J = 7.6$ Hz, 1H, N–H), 5.90 (app t, $J = 6.2$ Hz, 1H, H-1), 5.37 (app s, 1H, H-4), 5.26 (d, $J = 11.0$ Hz, 1H, H-3), 4.17 (dd, $J = 5.4$, 11.2 Hz, 1H, H-2), 4.13–4.03 (band, 3H, H-5, 6a, 6b), 2.16 (s, 3H, –CH_3), 2.10 (s, 3H, –CH_3), 2.08 (s, 3H, –CH_3), 2.02 (s, 3H, –CH_3). ^{13}C NMR (100 MHz, $CDCl_3$): δ 171.5, 170.6, 170.2, 75.6, 69.6, 67.0, 66.9, 61.5, 56.8, 23.2, 20.7, 20.6. ESI-MS: calcd for $C_{14}H_{20}N_4O_8$: *m*/*z*: 395.1179 $[M+Na]^+$; found: 395.1186 $[M+Na]^+$.

2.1. Crystal structure analysis

Colorless and transparent crystals of **1** were obtained by slow evaporation from a EtOAc–petroleum ether (1:1) solution. A suitable crystal of size (0.09×0.13×0.2 mm) was checked for extinction under a polarizing microscope and then mounted on a BRUKER AXS SMART APEX CCD diffractometer[3] with a crystal to detector distance of 6.06 cm. The data were reduced using SAINT PLUS[3] and the structure was solved by direct methods and refined using SHELXL[4] to an *R* value of 0.065. The hydrogen atoms were located by using the riding model with H-atoms in geometrically calculated positions, while all the nonhydrogen atoms were refined anisotropically (Table 1). The absolute configuration of **1** could not be determined from the X-ray data.

Table 1. Experimental details

Crystal data	
Chemical formula	$C_{14}H_{20}N_4O_8{\cdot}H_2O$
Chemical formula weight (M_r)	390.3
Cell setting, space group	Monoclinic, $P2_1$
a, *b*, *c* (Å)	8.588 (5), 12.707 (8), 8.773 (5)
β (°)	93.613 (11)
V (Å^3)	955.57 (13)
Z	2
D_x (Mg m^{-3})	1.35
Radiation type	Mo Kα
No of reflections for cell parameters	3709
θ range (°)	2.3–27.0
Temperature (K)	293 (2)
Crystal form, color	Block, white
Crystal size (mm)	0.09×0.13×0.2
Data collection	
Diffractometer	*SMART APEX* CCD area detector
Data collection method	ϕ scan
No of measured, independent and observed reflections	7015, 3709, and 2968
Criterion for observed reflections	$I > 2\sigma(I)$
R_{int}	0.024
θ_{max} (°)	25.0
Range of *h*, *k*, *l*	$-10 \rightarrow 9$, $-16 \rightarrow 15$, $-11 \rightarrow 11$
Absorption correction	SADABS
Extinction correction	None
Refinement	
Refinement on	F^2
R, *wR*, *S*	0.065, 0.192, 1.028
No of reflections and parameters used in refinement	3709 and 319
H-atom treatment	Riding model
Weighting scheme	$w = 1/\sigma^2(F_0^2)$
$\Delta\rho_{max}$, $\Delta\rho_{min}$ (e Å^{-3})	0.418, −0.458

3. Results and discussion

Compound **1** was characterized initially by ^{1}H and ^{13}C NMR spectroscopies. Unambiguous assignments of the ^{1}H and ^{13}C resonances of **1** were possible with the aid of ^{1}H–^{1}H correlation spectroscopy (COSY) and ^{1}H–^{13}C heteronuclear multiple quantum coherence (HMQC) experiments. The presence of anomeric acetamido substituent resulted in a significant upfield shift of ^{13}C resonance of anomeric carbon to 75.5 ppm. The axial configuration of the acetamido substituent is also inferred from the *J* value corresponding to H-1$_e$–H-2$_a$ of 4.5 Hz, which was obtained after D_2O exchange of the acetamido NH proton. The $^4C_1$ conformation was ascertained from the coupling constants $J_{2,3}$ of 11.1 Hz, which indicates the diaxial orientation of H-2 and H-3 protons. The antiperiplanar orientation of H-4 and synclinal orientation of H-2, with respect to *endocyclic* oxygen were also considered useful to establish the $^4C_1$ conformation of the pyranose ring. ^{1}H–^{1}H coupling constant analyses of **1** in $CDCl_3$ show that H-4$_e$–H-5$_a$ *J* value is nearly nil, whereas that for H-1$_e$–H-2$_a$ is 4.5 Hz. In line with reports[5,6] on solution phase characteristics of galactopyranosyl derivatives, we infer that the $^4C_1$ conformation is preserved in the solution phase for galactopyranosyl derivative **1**.

Single crystal X-ray structural analysis revealed a number of molecular and supramolecular features of **1** in the solid state. Crystals of **1**, suitable for X-ray analysis, were obtained upon slow evaporation of a solution of **1** in EtOAc–petroleum ether solution. Compound **1** (Fig. 1) crystallized in the monoclinic space group $P2_1$ with two molecules comprising a unit cell. The *ORTEP* of **1** is given in Figure 2. All significant bond distances, bond angles, and torsion angles are listed in Tables 2 and 3.

The molecule adopts nearly an ideal chair conformation as evidenced from the Cremer–Pople puckering parameters[7] $Q = 0.560$ Å, $\theta = 1.47°$, and $\varphi = 345.58°$. The nearly perfect chair conformation is also reflected with torsion angles of the substituents at neighboring carbons within the pyranose ring in synclinal orientations. The α-configuration of the anomeric center is identified from the torsion angle C5–O5–C1–N1 66.7 (5)° and the valence bond angles in the sequence C5–O5–C1–N1, which are 114.4 (0.2)° and 112.4 (0.3)°. The

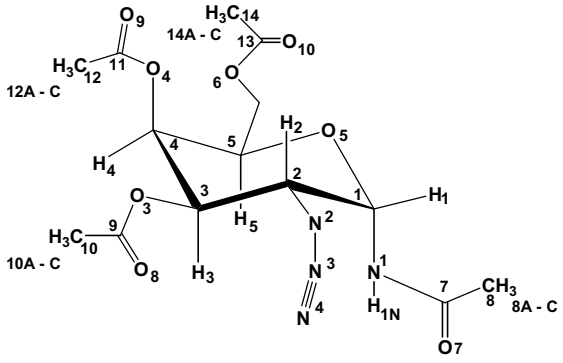

Figure 1. Molecular structure of **1** along with atom numbering.

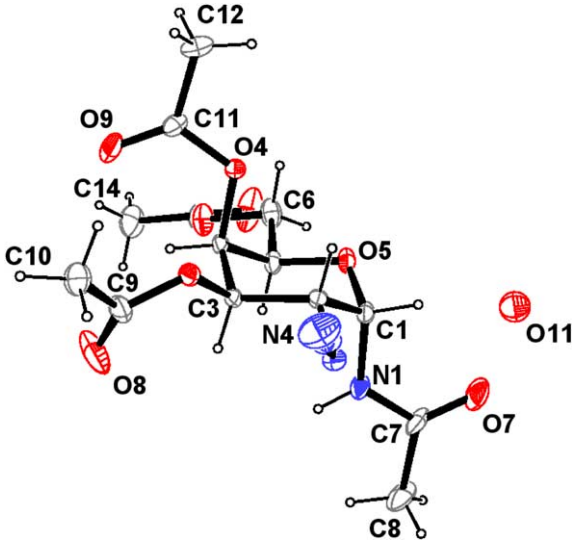

Figure 2. *ORTEP* of **1** with the displacement ellipsoids at 10% probability level.

Table 2. Selected bond lengths and bond angles for **1** (estimated standard deviations in parantheses)

Bonds	Length (Å)	Bonds	Angle (°)
C1–C2	1.522 (4)	O5–C1–C2	109.2 (2)
O5–C1	1.434 (4)	C3–C2–C1	110.8 (2)
C3–C2	1.532 (3)	C3–C2–N2	110.8 (2)
C2–N2	1.467 (5)	C1–C2–N2	108.9 (2)
N2–N3	1.199 (5)	N2–N3–N4	173.4 (5)
N3–N4	1.128 (7)	C4–C3–C2	111.2 (2)
C3–C4	1.511 (4)	O3–C3–C2	106.2 (2)
O3–C3	1.440 (3)	C3–C4–C5	109.5 (2)
C4–C5	1.525 (4)	O4–C4–C3	109.3 (2)
O4–C4	1.443 (3)	O5–C5–C4	110.6 (2)
C5–C6	1.487 (6)	O5–C5–C6	104.5 (3)
O5–C5	1.428 (3)	C5–C6–O6	106.9 (3)
C6–O6	1.453 (5)	O3–C9–C10	111.2 (4)
O3–C9	1.330 (5)	O3–C9–O8	122.6 (5)
C9–O8	1.176 (7)	C10–C9–O8	126.0 (4)
C9–C10	1.512 (7)	O4–C11–O9	122.6 (4)
O4–C11	1.351 (4)	O4–C11–C12	111.4 (4)
O9–C11	1.212 (6)	O9–C11–C12	125.9 (4)
C11–C12	1.488 (6)	C6–O6–C13	117.9 (4)
C13–O6	1.293 (6)	O10–C13–O6	121.2 (4)
C13–O10	1.197 (7)	O10–C13–C14	125.4 (5)
C13–C14	1.492 (8)	N1–C1–C2	113.1 (3)
N1–C1	1.434 (4)	N1–C7–O7	121.9 (4)
N1–C7	1.333 (5)	O7–C7–C8	123.1 (4)
C7–O7	1.205 (6)	N1–C7–C8	114.9 (5)
C7–C8	1.522 (7)	C4–C3–C2	111.2 (2)

Table 3. Selected torsion angles for **1** (estimated standard deviations in parantheses)

Bond	Torsion angle (°)
C5–O5–C1–N1	66.7 (3)
C5–O5–C1–C2	−59.6 (3)
C1–O5–C5–C4	60.8 (3)
C1–O5–C5–C6	−173.7 (2)
C7–N1–C1–O5	94.2 (4)
C1–N1–C7–O7	1.13 (7)
C1–N1–C7–C8	−179.6 (4)
C2–C3–C4–C5	52.8 (3)
C4–C3–C2–C1	−53.2 (3)
C4–C3–C2–N2	−174.3 (2)
O5–C1–C2–C3	54.3 (3)
C3–C4–C5–C6	−174.1 (2)
C3–C2–N2–N3	−86.8 (4)
O5–C5–C6–O6	173.6 (2)
C4–C5–C6–O6	−64.5 (4)
C2–N2–N3–N4	174.0 (4)

presence of 1-acetamido group in axial orientation is also clear from the torsion angles N1–C1–C2–N2 of 50.4 (0.3)° and N1–C1–C2–H2 of 168.8 (0.2)°. The methyl group in 1-acetamido substituent adopts an *anti* orientation with respect to the pyranose ring (torsional angle C1–N1–C7–C8 = −179.6 (0.4)°. The *anti* orientation of the methyl group was observed for those in the *O*-acetyl substituent also. The torsion angles O5–C5–C6–O6 of 173.4 (0.2)° and C4–C5–C6–O6 of −64.5 (0.4)° show that the 6-*O*-acetyl substituent adopts a *trans–gauche* arrangement with respect to the pyranose ring. The

Table 4. Hydrogen bond data for D–H···O bonds

	D–H···A	H···A (Å)	D···A (Å)	∠D–H–A (°)
(1)	N(1)–H(1N)···O(11)	2.026	2.836 (6)	156.5
(2)	C(8)–H(8b)···O(11)	2.422	3.278 (9)	148.2
(3)	C(10)–H(10b)···O(11)	2.538	3.467 (8)	162.7
(4)	C(10)–H(10a)···O(5)	2.666	3.450 (7)	139.1

Symmetry code: (1) and (2) $x+1, +y-1, +z-1$; (3) $x+1, +y-1, +z$; (4) $-x+2, +y-1/2, -z+1$.

2-azido moiety orients in a nearly linear fashion with N2–N3–N4 angle being 173.4 (0.5)°.

A molecule of water cocrystallized with **1**, even while the uptake of water molecule, presumably moisture oriented, would have occurred during the crystallization process. The water molecule is located at a distance well poised for strong N–H···O hydrogen bonding and C–H···O interactions.[8] It is to be noted that while water of hydration is common in free hydroxyl group containing sugar derivatives, the presence of the water molecule in protected derivatives is rare.[9] The supramolecular organization in the crystalline lattice of **1** is dominated primarily by noncovalent interactions arising from this inadvertently entrapped water molecule. The C–H···O bonds were considered based on the distance criterion (<2.7 Å) and the angle constraint CHO > 120° and were identified by PARST97.[10] The details of the hydrogen bonds and their symmetry parameters are given in Table 4.

The water molecule participates essentially in: (i) N–H···O (N1–H1$_N$···O11) interaction; (ii) C–H···O (C8–H8b···O11) interaction with the same molecule involved in the N1–H1$_N$···O11 interaction, and (iii) C–H···O (C10–H10···O11) interaction with another molecule of **1** (Fig. 3). By the way of involving two molecules to initiate the above three interactions, the water molecule is sandwiched between these two molecules when viewed through the axis perpendicular to the screw axis. Upon extending the molecules in stacks in the *a* direction, an open channel evolves and the water molecules reside inside the channel. The N–H···O and C–H···O interactions interconnect adjacent molecules throughout the channel and thereby contribute to stabilize the crystal lattice. A stereoview of the channel entrapped with a water molecule is shown in Figure 4. In addition to the above mentioned network, we have also observed short intermolecular distances between the water oxygen O11 and O7, O10, N1 in a distance of 2.608 (8), 2.500 (6), 2.836 (6) Å, respectively, suggestive of hydrogen bonding interactions involving the hydrogens of the water molecule. These interactions, however, could not be located from the X-ray data.

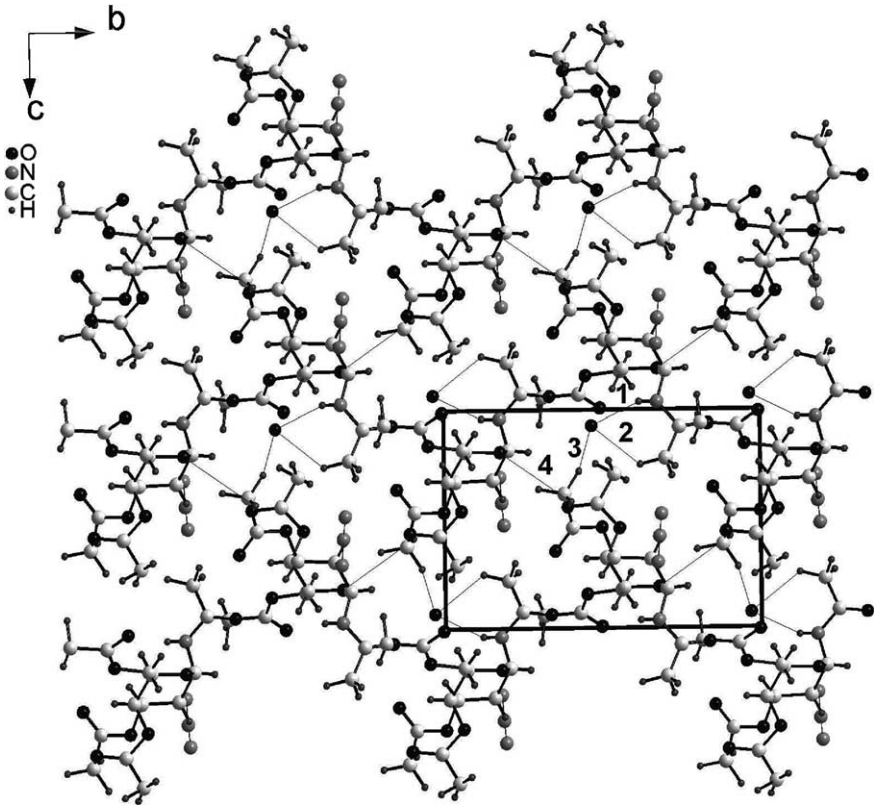

Figure 3. N–H···O and C–H···O interactions (packing along axis *a*). The numbers denote the following interactions: (1) N(1)–H(1N)···O(11); (2) C(8)–H(8b)···O(11); (3) C(10)–H(10b)···O(11); and (4) C(10)–H(10a)···O(5).

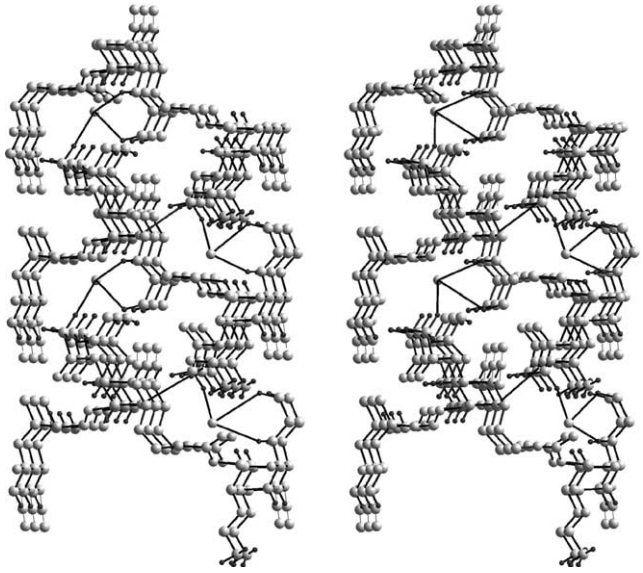

Figure 4. A stereoview of N–H···O and C–H···O interactions mediated by a water molecule (packing along axis *a*).

Apart from N–H···O and C–H···O interactions mediated by the entrapped water molecule, an additional C–H···O interaction, namely, C10–H10a···O5, involving the endocyclic pyranose ring oxygen, was also evident from the crystal structure analysis. The hydrogen bonding ability of the *endocyclic* O5 oxygen is a common feature in free sugar derivatives.[11] The H···O distance of C10–H10a···O5 (2.666 Å) was found to be longer when compared to the distances C8–H8b···O11 (2.422 Å) and C10–H10b···O11 (2.538 Å). Considering the corresponding D–H···O angles as given in Table 4, the C10–H10a···O5 interaction may be considered relatively weaker.

4. Conclusion

The NMR spectroscopic and crystallographic analyses of derivative **1**, a product of the widely used azidonitration of glycals, were performed. While these characterizations allowed assessing the molecular features of **1**, an interesting outcome of the structural analysis was the importance of the roles played by weak and strong interactions in stabilizing the molecular packing. It is very likely that the relatively strong N–H···O interaction, followed by the C–H···O interactions, as mediated primarily by the entrapped water molecule, determine the extent of noncovalent interactions in **1**. Subtle coordination of these 'strong' and 'weak' interactions not only stabilize the nearly perfect $^4C_1$ conformation of the molecule, but also the overall molecular packing.

5. Supplementary material

The data were deposited at the Cambridge Structural database (Accession number CCDC 227824). Copies of this information can be obtained free of charge from The Director, CCDC, 12 Union Road, Cambridge CB21EZ, UK (fax: +44-1223-336033; e-mail: deposit@ccdc.cam.ac.uk or http://www.ccdc.cam.ac.uk).

Acknowledgements

We thank Department of Science and Technology, India, for data collection on the CCD facility setup under the IRHPA-DST program. N.J. thanks Department of Science and Technology, India, for a financial support.

References

1. Lemieux, R. U.; Ratcliffe, R. M. *Can. J. Chem.* **1979**, *57*, 1244–1251.
2. For example; (a) Pozsgay, V. *J. Org. Chem.* **1999**, *64*, 7277–7280; (b) Seeberger, P. H.; Roehrig, S.; Schell, P.; Wang, Y.; Christ, W. *J. Carbohydr. Res.* **2001**, *328*, 61–69.
3. Bruker SMART and SAINT, Bruker AXS Inc., Madison, Wisconsin, USA, 1998.
4. Sheldrick, G. M. SHELXS97 and SHELXL97, University of Göttingen, Germany, 1997.
5. Mallet, A.; Mallet, J.-M.; Sinay, P. *Tetrahedron: Asymmetry* **1994**, *5*, 2593–2608.
6. Liberek, B.; Dabrowska, A.; Frankowski, R.; Matuszewska, M.; Smiatacz, Z. *Carbohydr. Res.* **2002**, *337*, 1803–1820.
7. Cremer, D.; Pople, J. A. *J. Am. Chem. Soc.* **1975**, *97*, 1354–1358.
8. Desiraju, G. R. *Acc. Chem. Res.* **1996**, *29*, 441–449.
9. (a) Buist, P. H.; Behrouzian, B.; MacIsaac, K. D.; Cassel, S.; Rollin, P.; Imberty, A.; Gautier, C.; Perez, S.; Genix, P. *Tetrahedron: Asymmetry* **1999**, *10*, 2881–2889; (b) Tomić, S.; van Eijck, B. P.; Kojić-Prodić, B.; Kroon, J.; Magnus, V.; Nigović, B.; Laćan, G.; Ilić, N.; Duddeck, H.; Hiegemann, M. *Carbohydr. Res.* **1995**, *270*, 11–32.
10. Nardelli, L. J. *Appl. Crystallogr.* **1995**, *28*, 659.
11. Jeffrey, G. A.; Mitra, J. *Acta Cryst.* **1983**, *B39*, 469–480.